Experimental testing on the influence of shaft rotary lip seal misalignment for a marine hydro-kinetic turbine.

HAND, B.P., ERDOGAN, N., MURRAY, D., CRONIN, P., DORAN, J. and MURPHY, J.

2022

Experimental testing on the influence of shaft rotary lip seal misalignment for a marine hydro-kinetic turbine

Brian P. Hand[a,*], Nuh Erdogan[b], Dónal Murray[a], Patrick Cronin[c], John Doran[d], Jimmy Murphy[a]

[a] *Marine and Renewable Energy Centre, University College Cork, Cork, Ireland*
[b] *School of Engineering, Robert Gordon University, Aberdeen, UK*
[c] *Ocean Renewable Power Company, Dublin, Ireland*
[d] *The Bryden Centre, Letterkenny Institute of Technology, Letterkenny, Donegal, Ireland*

Abstract

Tidal energy has received considerable attention over the past decade due to its predictability and high power density. The research in the tidal turbine area has concentrated primarily on the improvement of the energy conversion efficiency. In contrast, the testing of the tidal turbine's mechanical components has received less attention. In particular, the reliable operation of rotary seals is crucial to prevent water ingress into mechanical and electrical components. This paper outlines an experimental test campaign to investigate the effect of shaft misalignment. Both instantaneous temperature and pressure measurements were recorded from two rotary seals. It was shown the temperature inside the aligned seal increased until the seal chamber pressure became equal with the inlet water pressure. The wear on the lip seal rings was examined and the difference found to be between 3.28% and 19.61%. Inspection of the seal liners, showed the presence of strong wiping effects for the misaligned seal with maximum track width differences of between 52.94% and 97.60% being noted. The misaligned seal liner experienced wider wear tracks but were not as deep as the aligned seal with differences of between 37.55% and 103.13% being recorded.

Keywords: Tidal Energy, Hydro-kinetic turbine, lip seal, testing

1. Introduction

The increasing prices of fossil fuels and the growing demand for energy coupled with the acceptance that global warming of the planet is occurring is driving the development of new renewable energy devices [1, 2]. Tidal energy has an enormous potential to generate electricity from marine tidal currents. The European Commission estimates that ocean energy could supply 15% of Europe's electricity demand by 2050 [3, 4]. However, a major obstacle in the further development of this technology in comparison to other renewable energy sources is its economic viability and ultimately its high Levelised Cost of Energy (LCOE) [5]. The challenges which need to be addressed involve increasing the performance and reliability of ocean energy subsystems [6, 7].

In particular, the advancement of the tidal system drivetrain rotary shaft seals to be operable in a seawater environment is important [8–10]. The tidal turbine mechanical components must be enclosed in an environment and is usually achieved using a rotary seal on the drive shaft of the turbine [11]. This rotary seal is crucial for a tidal turbine to operate under hydrostatic pressure, especially for the connection between the drive shaft and generator [12]. To date, some research has been undertaken to improve and study the design of tidal turbine rotary seals. Lee et al. [13] conducted accelerated wear tests of a fluorocarbon elastomer for life prediction of seals. Nakanishi et al. [14] introduced a new type of shaft seal with two hydrated lips to separate water and atmosphere with low fictional torque. Honda et al. [15] examined the

* Corresponding author
Email address: brianpeterhand@gmail.com (Brian P. Hand)

application of bio-inspired material for a shaft seal covering a low range under water environment. De Cal [16] examined the vibration response due to the misalignment of a tidal turbine shaft. It was found that vibration monitoring in two planes is needed to determine the cause of failure. In the shipping industry, which presents a similar design problem to a tidal turbine, a set of rotary lip seals are placed at both ends of the stern tube to prevent lubricant leaking and seawater entering the stern tube enclosing the propeller shaft [17]. In comparison to a ship propeller shaft, a tidal turbine shaft will experience larger deflection when loaded. This paper presents the test results of employing a ship rotary shaft seal configuration for a submerged tidal turbine. From an extensive literature review, this is the first time, this type of rotary shaft seal has been tested for a hydro-kinetic turbine application. In particular, the performance of the rotary shaft seal in an aligned and misaligned position will be examined to consider the influence of turbine shaft deflection.

This paper is organised as follows: The development of the experimental test rig, methodology and instrumentation is outlined in Section 2. Section 3 details the results of 952 hours of testing conducted over a 10 month period. Firstly, the pressure and temperature results from inside the rotary seal's chambers during operation are presented. Secondly, the results of a wear rate inspection of the rotary lip seals and the shaft liners are discussed. Conclusions from this test campaign follow in Section 4.

2. Experimental setup

An experimental test rig was designed and manufactured to test the rotary seal configuration as shown in Figure 1.

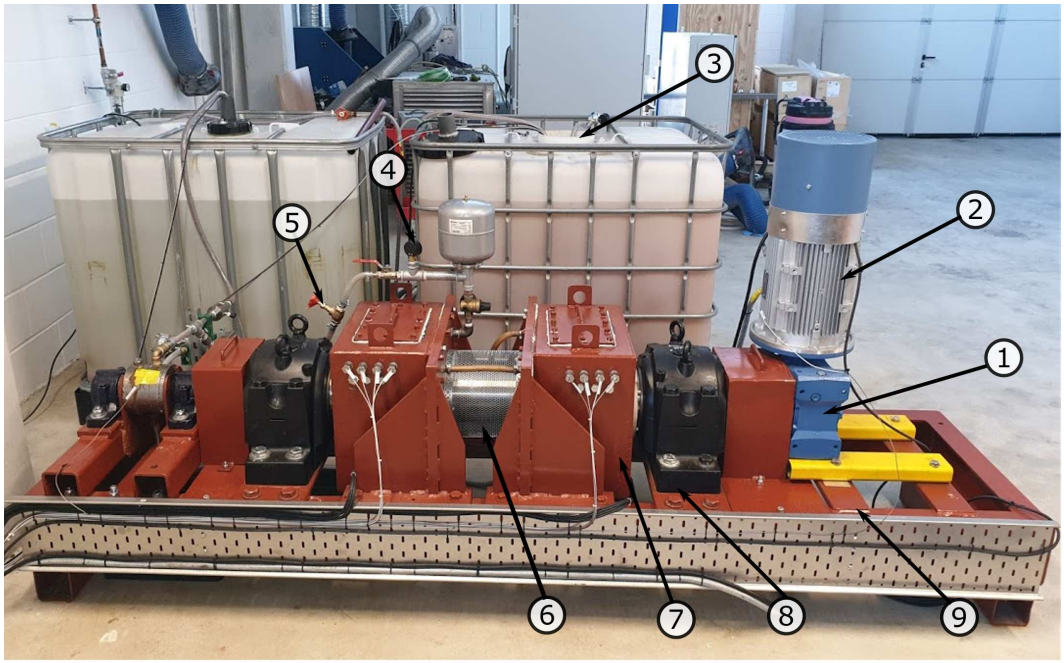

Figure 1: Configured rotary seal experimental test rig with labelled components.

The rig consists of steel frame to support the experimental test components. Attached to the frame is a

3-phase, 7.5 kW, 1450 RPM induction motor is used to rotate a driveshaft through a gearbox with a ratio of 10:1. This motor is used to emulate the drive force from a hydro-kinetic turbine. The motor is fed by a Techniques Unidrive SP3403 variable speed drive that implements a closed-loop speed control with an incremental encoder. The motor was cooled by a coupled 145 W axial fan. The gearbox is attached to the driveshaft through a flexible Dunlop F80 tyre coupling to accommodate any misalignment between the two connecting shafts. The driveshaft is supported onto the frame using two SKF tapered roller bearings with plummer black housings (SNL 3134) with an internal bore of 170 mm. Positioned at the opposite sides of the midpoint of the driveshaft are two sealed steel boxes. Within each box was a Simplex lip type rotary seal as shown in Figure 2.

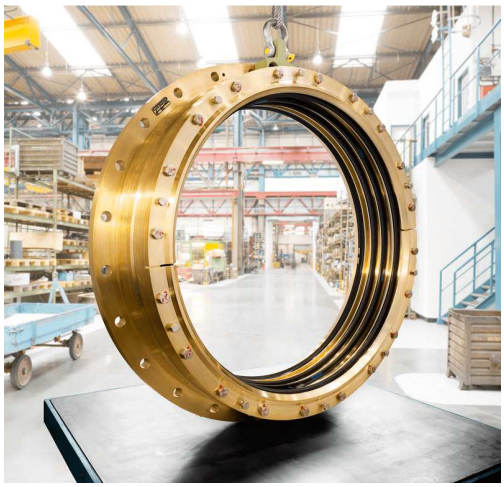

Figure 2: Simplex seal [18].

The seal lips are running on a corrosion resistant seal liner which is fixed onto the driveshaft. The liner material is stainless steel and has a tungsten carbide coating. Each of the Simplex seals had three grease chambers with incorporated lip seals which were in contact with the seal liner. The lubricating grease used this experiment is Klüber Isoflex Topas. One of the Simplex seals was aligned parallel to the driveshaft axis, while the other was misaligned by 1° to its maximum deflection to emulate turbine shaft deflection as depicted in Figure 3.

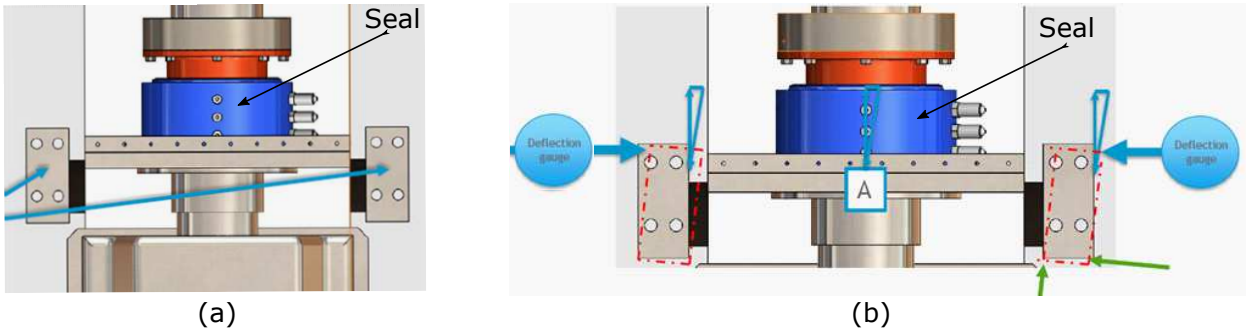

Figure 3: Seal alignment with respect to drive shaft axis (a) aligned (b) misaligned.

This was facilitated in order to compare the wear rates of the two Simplex seals are shown in Figure 4.

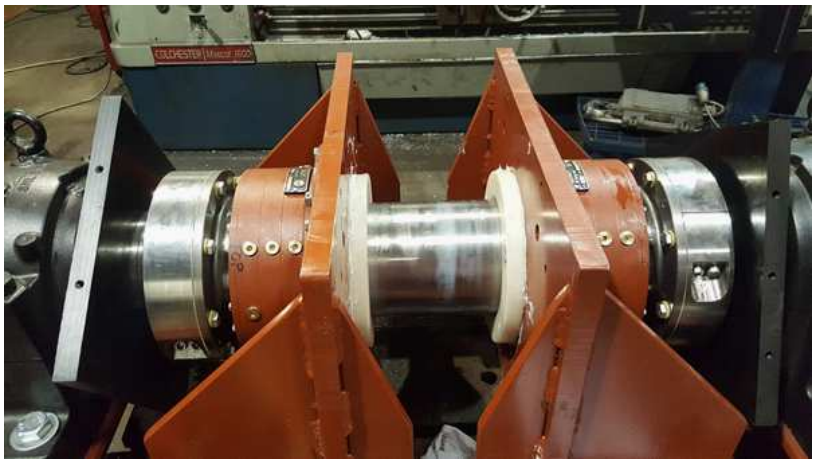

Figure 4: Aligned (left) and misaligned (right) Simplex seal assembly. Note: seal steel boxes removed in this image.

To maximise, the wear rate, the driveshaft speed was set to its maximum design speed of 144 RPM. The two Simplex seals were tested under 1 bar pressure relative to atmosphere to replicate the 10 m water depth pressure of the marine hydro-kinetic turbine application. To achieve this pressure, a 750 W Draper submersible pump was employed to pump water at room temperature from an adjacent storage water tank through the two sealed tanks and back to this storage tank to be recycled. The water inlet pressure was regulated using an incorporated manual gate valve and a pressure dial gauge, which are shown in Figure 1.

2.1. Instrumentation

Each Simplex seal consists of three chambers and can be accessed by a port as shown in Figure 5a. Within each chamber is two lip seals as shown in Figure 5b, which are in contact with a cylindrical liner surrounding the drive shaft. The lip seal closest to the water pressure which in this case is lip seal 4 is pressed strongly against the seal liner.

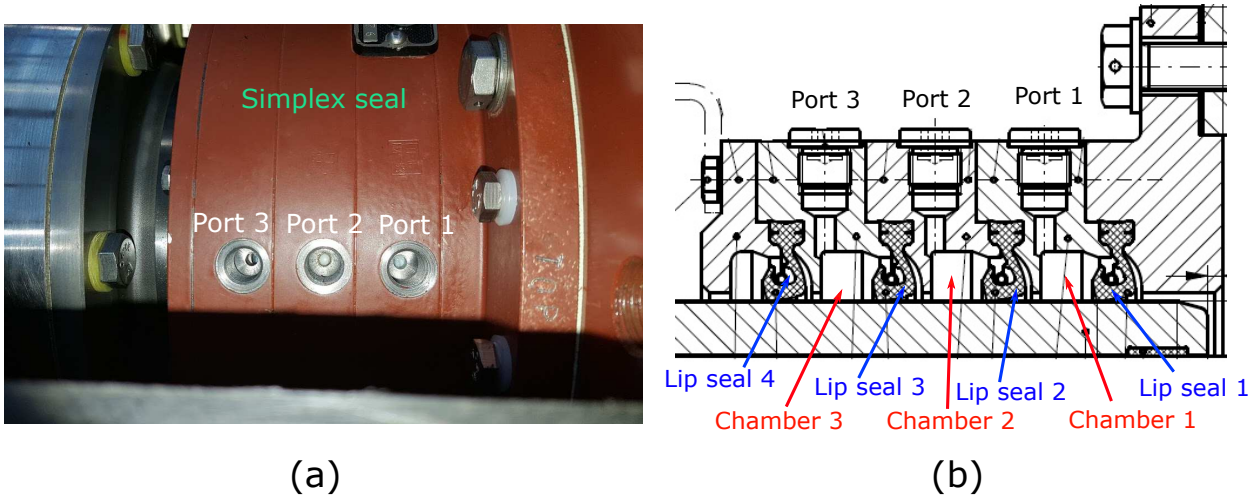

Figure 5: (a) Simplex seal chamber access ports (b) seal sectional view.

Both pressure and temperature sensors are inserted into the access ports. As well, the pressure and temperature sensors are installed inside the seal boxes. Figure 6 shows the pressure and temperature sensors inserted into the Simplex seal chamber ports.

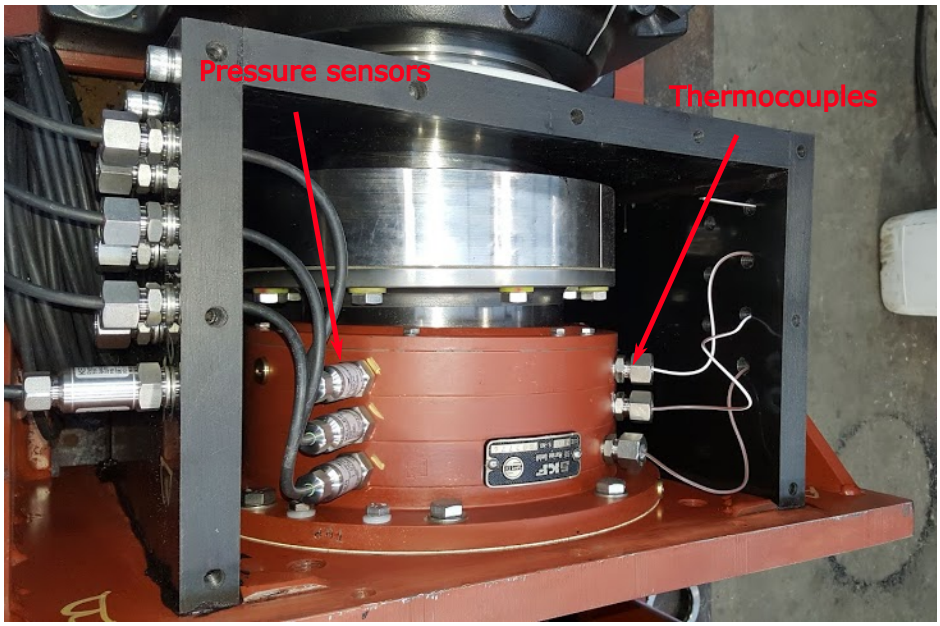

Figure 6: Pressure and temperature sensors installation in the Simplex seal's chambers.

In total, there were 8 pressure and 8 temperature measurements recorded during continuous operation. Temperature measurements were made using Type T thermocouples, with a temperature range of $-200°C$ to $200°C$ and an accuracy of $\pm 0.75\%$. Pressure measurements were made using Keller 4-20 mA PAA-23SY pressure transducers with an accuracy of $\pm 0.25\%$ full scale [19]. A data acquisition system was also developed to monitor the test operation and to collect the data using a Mitsubishi PLC and its corresponding I/O modules. All instrumentation, control and power equipment were installed in an enclosed panel. Figure 7 shows a schematic of the position of the pressure and temperature sensors in the two Simplex seals in plan view. The two seals are denoted as the Aligned Seal and the Misaligned Seal. The misaligned seal is located near the motor and is denoted as the Motor side in the Figure 7.

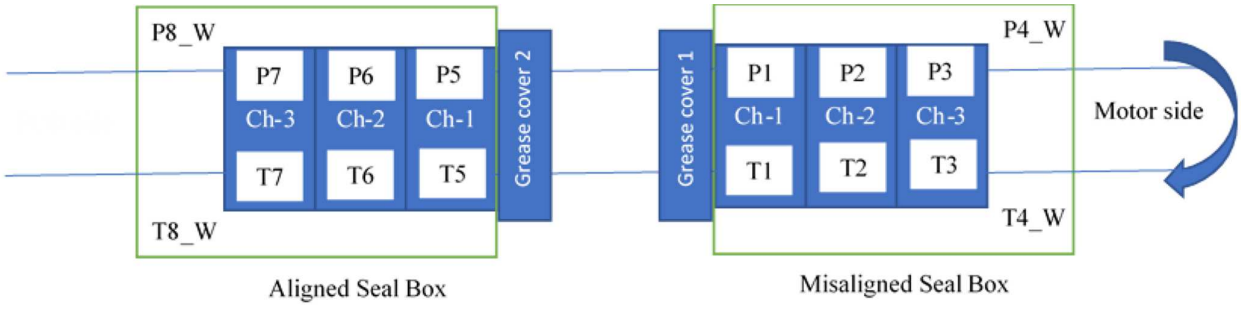

Figure 7: Orientation of the Simplex seals, the pressure and temperature sensors installed in the seals.

The data acquisition software was started and measurements from the pressure and temperature sensors were recorded in one second resolution. Each test was run continuously for at least 8 hours. After the test had been completed, the motor was stopped and the recorded sensor data was saved for post-processing. Testing was conducted over a period of 10 months using the test rig.

3. Results

3.1. Pressure and temperature measurements

The pressure and temperature measurements were recorded in the chambers of the aligned and misaligned seals. The water temperature and pressure surrounding the seals in both cases were recorded also. The recorded experimental data is availible at [20]. Figure 8 shows the variation in the chamber pressure for the aligned and misaligned seals on starting the testing campaign. The chamber pressures in the aligned are higher compared to those of the misaligned seal. In particular, chamber 3 in the aligned seal, which is closest to the water experiences the highest recorded pressure.

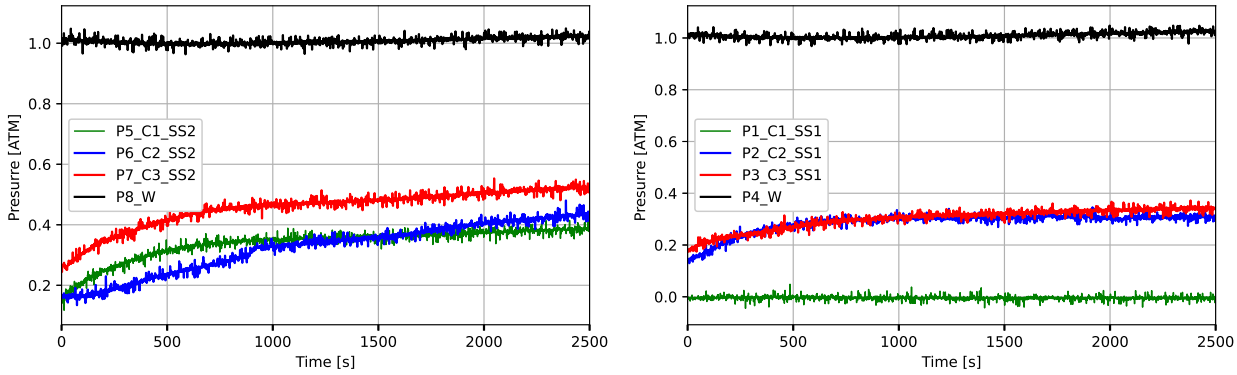

(a) (b)

Figure 8: Pressures in the chambers at the startup of testing: a) the aligned seal, b) the misaligned seal.

Similar to the pressure results, the aligned seal experiences the largest increase in temperature in Figure 9. In particular, chamber 2, which is between chamber 1 and chamber 3, experiences the greatest fluctuations in the temperature and exceeds 55°C. It is believed chamber 2 experiences the highest temperature here due to the bedding in process of the lip seals on the seal liner. This is to be expected as chamber 2 is located centrally over the four lip seals. At the start up phase, the lip seals will encounter the greatest friction against the liner surface. This in turn, generates heat and is transferred through the chambers and in particular chamber 2, raising its in chamber temperature greatly. It will be shown in Section 3.2.2 the wear on the surface of the seal liner due to the contact of the seal lips.

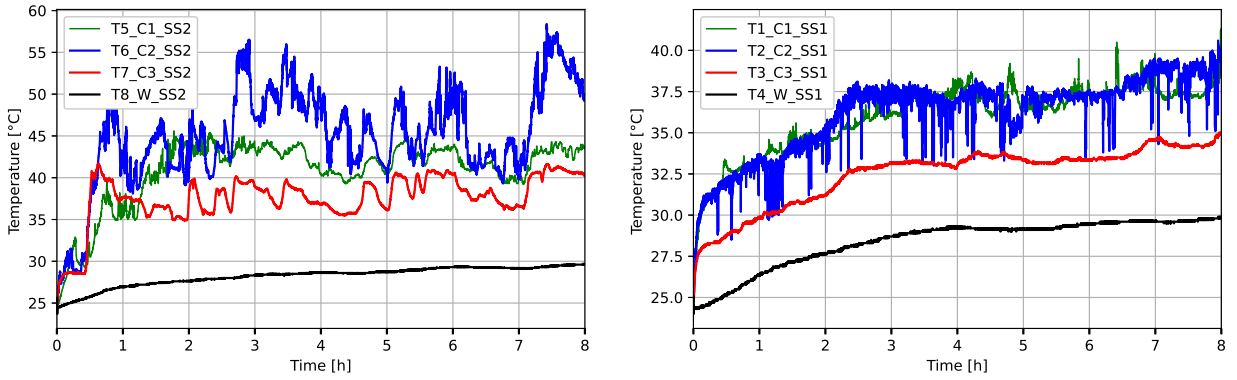

(a) (b)

Figure 9: Temperatures in the chambers at the startup of testing: a) the aligned seal, b) the misaligned seal.

After 100 hours of testing the pressure variation in the two seals can be observed in Figure 10. It is interesting to note the chamber 3 pressure in the aligned seal (Figure 10a) has increased considerably and is

close to the outside water pressure. This may suggest the first lip seal which is closest the pressurised water has started to decline in effectiveness. In contrast, the chamber pressures in the misaligned seal are much lower and are almost null. The would infer the lips are operating effectively with almost constant pressure in the misaligned seal chambers.

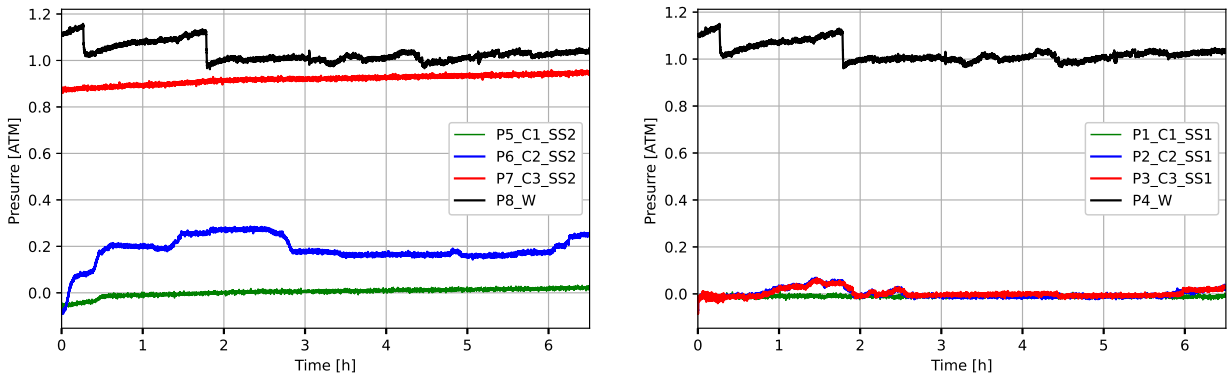

(a) (b)

Figure 10: Pressures in the chambers after 100 hours testing: a) the aligned seal, b) the misaligned seal.

Figure 11 displays the temperature variation within the seal chambers after 100 hours of testing. Chamber 3 in the aligned seal experiences the highest temperature of over 60°C. In contrast, in the misaligned seal case, chamber 3 experiences the lowest temperature relative to the other two seal chambers. It is interesting to see the temperatures in the aligned seal are higher when compared to the misaligned seal. It is postulated the higher temperatures experienced in the aligned seal is due to the higher friction between the sealing rings around the circumference of the liner when compared to the misaligned seal. The misaligned seal does not have a constant contact pressure and is distributed over a greater running area and will be discussed in more detail in Section 3.2.2.

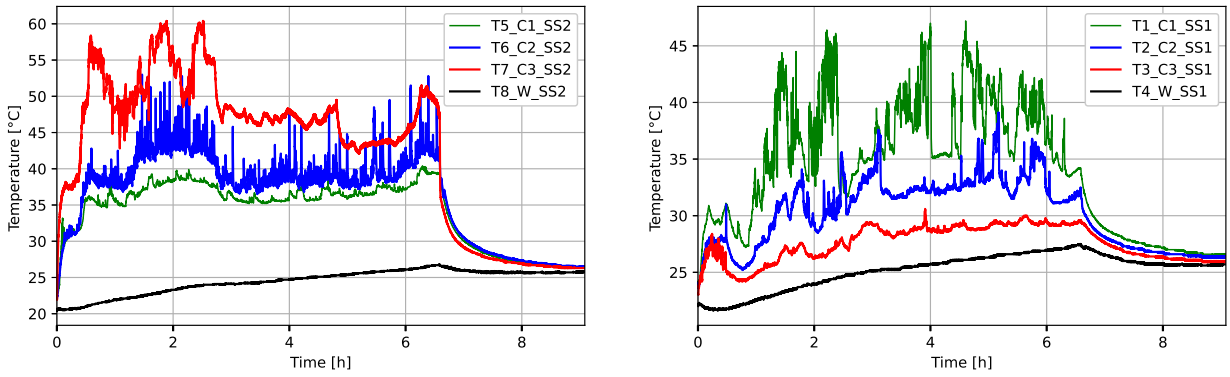

(a) (b)

Figure 11: Temperatures in the chambers after 100 hours testing: a) the aligned seal, b) the misaligned seal.

Figure 12 shows the pressure fluctuation within the chambers of the two seals after 350 hours of testing.

The pressure variation within the aligned seal in Figure 12a show a very similar behaviour to those after 100 hours of testing in Figure 10a. It is interesting to note the pressure in chambers 1 and 2 of the aligned seal, has increased by between 0.2 and 0.4 of one atmosphere. This maybe due the increased pressure witnessed in chamber 3 and an equalisation of pressure throughout the chambers, from chamber 3 to chamber 1. The change in the seal chamber temperatures after 350 hours of operation can be viewed in

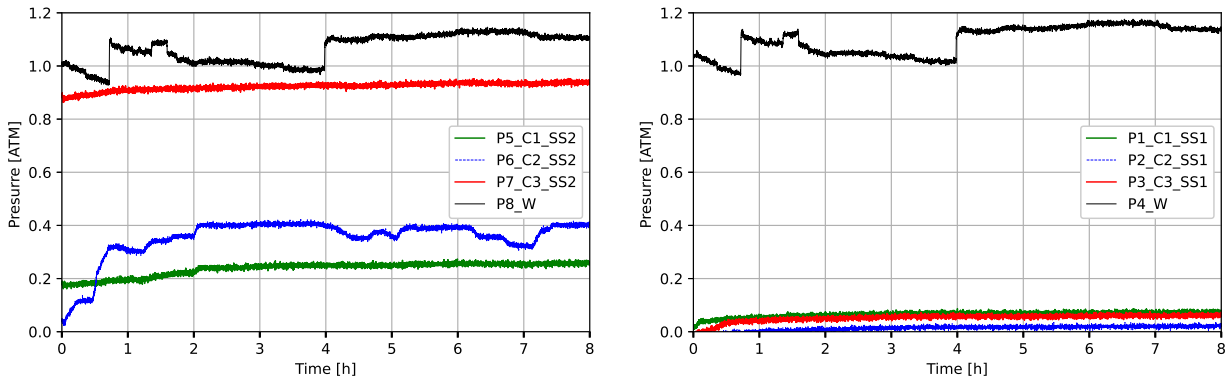

(a) (b)

Figure 12: Pressures in the chambers after 350 hours testing: a) the aligned seal, b) the misaligned seal.

Figure 13. Similar to the pressure measurement behaviour, the temperature readings are very similar to the measurements taken after 100 hours of operation. This would appear to imply that the system has stabilised at these pressures and temperatures after 100 hours. Chamber 2 experiences the highest temperatures for both the aligned and misaligned seal cases.

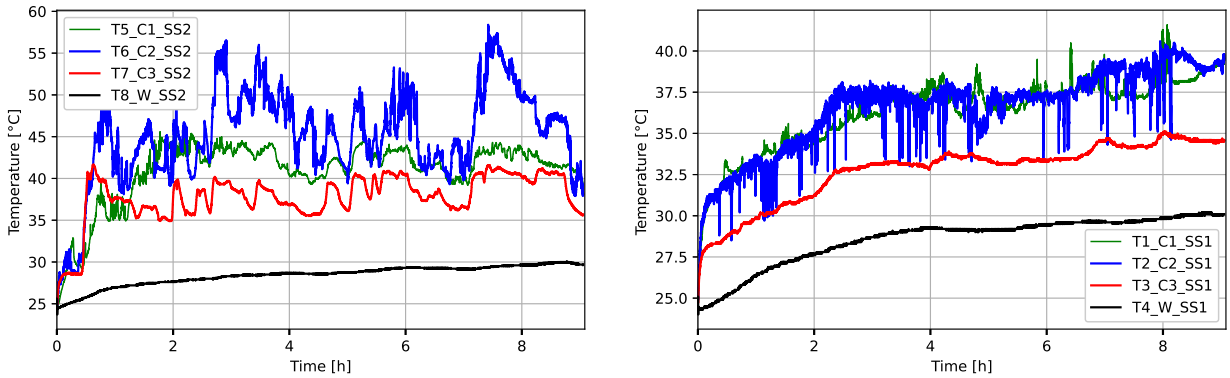

(a) (b)

Figure 13: Temperatures in the chambers after 350 hours testing: a) the aligned seal, b) the misaligned seal.

Figure 14 displays the pressure measurements taken from the seal chambers for the aligned and misaligned cases after 350 hours of testing. For the aligned seal in Figure 14a, it can be observed that the seal chamber pressures have become approximately equal to the water pressure surrounding the seal body. This would suggest the aligned seal has ceased being effective. Through much of the 8 hour run, the pressure within chamber 3 has exceeded the exterior water pressure and would suggest water is passing the first lip seal ring. It was found after 183 hours of testing, the aligned seal chamber 3 pressure became equal to the water tank pressure. In contrast, for the misaligned seal in Figure 14b, just the pressure inside chamber 3 has become equal to the water pressure around the seal body.

After 359 and 538 hours the pressure in chamber 2 and 1 for the aligned seal became equal to the tank pressure. This result suggests the seal maintained in an aligned position can prevent water ingress for 538 hours. As the seals are being tested for a submerged turbine application water ingress must prevented to the electrical generator. It is interesting to note the pressure in chamber 3 of the misaligned seal equalised the water pressure after 583 hours. This would infer that some shaft deflection could be beneficial in extending the sealing time provided by the seal system. It worth mentioning here the shaft in this testing was running

at maximum operational rotational velocity. Therefore, the time periods noted here would be longer in reality, as it is not expected the turbine will be operating at maximum rotational velocity continuously.

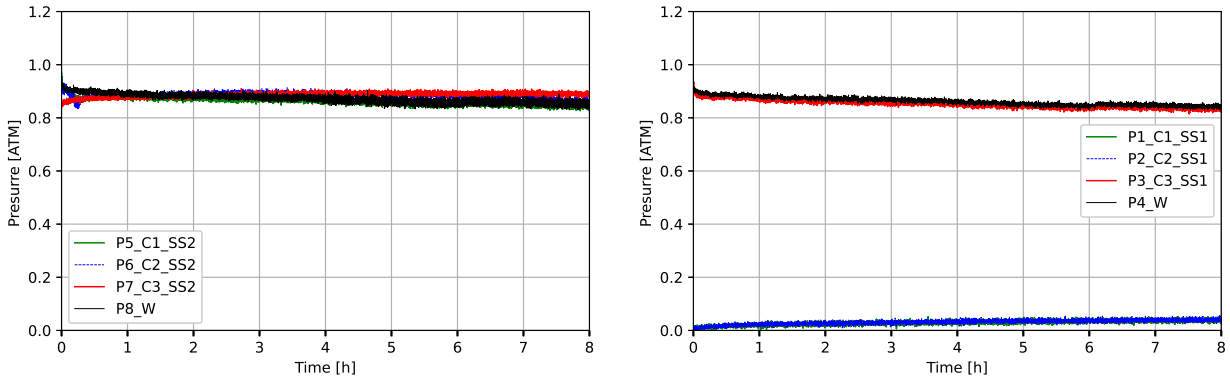

(a) (b)

Figure 14: Pressures in the chambers after 600 hours testing: a) the aligned seal, b) the misaligned seal.

Figure 15 shows the temperature variation in the two seals after 600 hours testing. It is interesting to observe in Figure 15a that the temperature range in the aligned seal has reduced considerably and is lower than the misaligned seal temperatures in Figure 15b. It is postulated this temperature reduction in the aligned seal chambers is due to the chamber pressures equalising with the inlet water pressure and a subsequent cooling effect. It is worth noting also in Figure 15a, that chamber 1 now experiences the highest temperature, which is furthest away from the cooler water being pumped through the system.

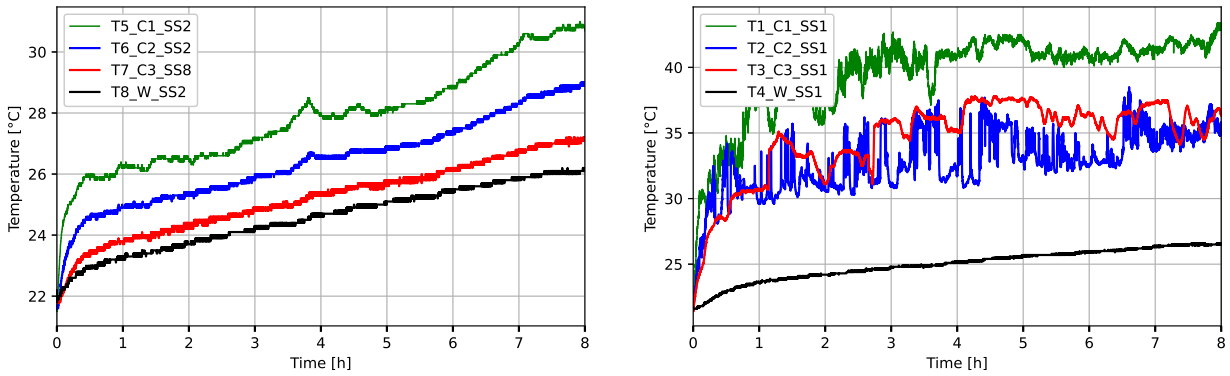

(a) (b)

Figure 15: Temperatures in the chambers after 600 hours testing: a) the aligned seal, b) the misaligned seal.

3.2. Wear inspection

After the pressure and temperature data was collected from the experimental test rig, it was disassembled to permit wear inspection of both the lip seals and the seal liners as shown in Figure 16.

Figure 16: Simplex seals and associated liners prior to wear inspection (a) aligned (b) misaligned.

3.2.1. Lip seals

The wear rate on the lip seal rings of the aligned and misaligned positions were examined. Table 1 shows the results of this analysis.

Table 1: Lip seal track wear width measurement in aligned and misaligned positions.

Lip seal ring	LS1	LS2	LS3	LS4	Mean	Standard deviation
Aligned position (mm)	4.2	3.2	3.0	4.6	3.8	0.8
Misaligned position (mm)	4.7	2.8	3.1	5.6	4.1	1.3
Difference (mm)	0.5	0.4	0.1	1	0.3	0.6
Percentage difference	11.24%	13.33%	3.28%	19.61%		

It was found the aligned position had a more consistent wear rate across its four lip seals compared the misaligned seal with a lower standard deviation. In the aligned and misaligned position, the lip seal (LP4) nearest to the water pressure experienced the highest wear rate. In the misaligned position, increased wear is experienced on three of the four lip seals, with lip seal 2 (LS2) experiencing less wear. It is postulated that this is due to the liner adjusted by 1° and therefore a higher force is applied to one side of the sealing rings. This occurrence is clearly seen in both LS1 and LS4 seals as illustrated in Figure 17. From Table 1, it can be seen the greatest difference in the lip seal wear was for LS4 at 19.61% and the lowest for LS3 at 3.28%. From an operational perspective, the deflection of the turbine shaft and the subsequent misalignment of the rotary seal will result in increased wear for the first and last sealing rings compared to the non-deflected scenario.

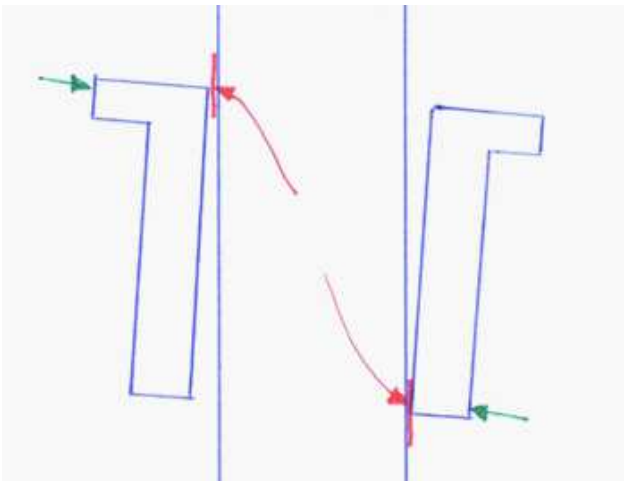

Figure 17: Illustration showing misaligned seal with increased contact at LS1 and LS4.

3.2.2. Seal liners

The surface of the seal liners were also inspected after the testing campaign and are shown in Figure 18.

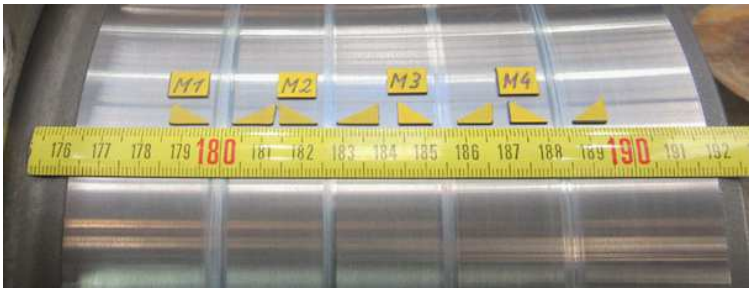

(a) Aligned position

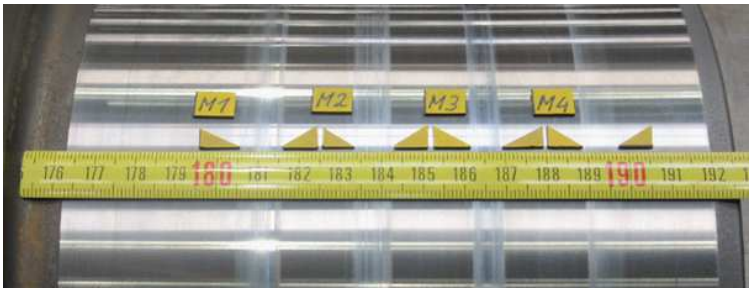

(b) Misaligned position

Figure 18: Track on the surface of the liner (a) aligned position (b) misaligned position.

It can be seen in Figure 18 that the lip seals left visible marks on the liners. It was expected that the track widths on the liner would be larger than the ones on the sealing rings. This is due to the ubiquitous run-out of the drive shaft or pressure fluctuations. In turn this produces wiping effects of the sealing rings on the liner. In Figure 18a, the wear tracks on the liner are clearly defined. On the other hand, the seal in the misaligned position as shown in Figure 18b, the tracks on the liner surface are less defined. It can also be observed in Figure 18 that there is significantly wider track widths on the misaligned liner when compared to its aligned state. Table 2 outlines the measurements of liner track widths and depths. The track depths

were measured using a digital microscope and the track widths were measured using a metric ruler.

Table 2: Liner track wear width and track wear depth in aligned and misaligned positions.

Lip seal ring	LS1	LS2	LS3	LS4
Aligned position track width (mm)	5	3.9	3.2	4.8
Misaligned position track width (mm)	5.2-8.6	3.8-7.2	4.1-9.3	6.0-10.3
Maximum difference	52.94%	59.46%	97.60%	72.85%
Aligned position track depth (μm)	6.34	3.827	4.116	8.266
Misaligned position track depth (μm)	2.026	2.617	2.862	2.764
Difference	103.13%	37.55%	35.94%	99.76%

It was determined that in the misaligned state the wiping effects are more stronger than in the aligned state. From Table 2, it can be seen that the track width differences are large with the maximum difference being found to be between 52.94% and 97.60%. Another striking point is the track depth. This is significantly lower in the misaligned state than in the aligned state. This is because the sealing rings around the circumference do not have a constant surface pressure (as with the ideally aligned seal) on the liner and the contact pressure is distributed over a wider running surface. As expected the greatest differences is noted for LS1 and LS4 with approximately 100% difference between the aligned and misaligned seal liner wear track depths encountered. It is worth highlighting here the shaft deflection was 1°, which is the maximum the turbine would experience during operation.

4. Conclusions

This paper outlines the results of an experimental testing campaign to examine the effect of drive shaft misalignment on the performance rotary lip seals. An experimental test rig was manufactured where two rotary lip seals were tested together in two different configurations, the first being aligned with the shaft axis and the other misaligned relative to the shaft axis to consider the effect of shaft deflection. The temperature measurements showed that the aligned seal experienced higher chamber temperatures compared to misaligned seal, when the chamber pressures in the aligned seal were below the inlet water pressure. Once the chamber pressures in the aligned seal equaled the inlet water pressure, the subsequent chamber temperatures reduced. The aligned seal became equal to the tank pressure in the descending order of chamber numbers (P7, P6, P5) after 183, 359, and 538 hours of operation, respectively. For the misaligned seal, only the outer chamber's pressure (P3) reached the tank pressure after 583 hours of operation.

After the testing had been completed, an inspection of the condition of the seal lips and the seal liners was conducted. It was found the two outer seal rings (LS1 and LS4) of the misaligned seal exhibited a higher wear rate than the equivalent seal rings of the aligned seal. The difference in wear rate was found to be between 3.28% and 19.61%.

Inspection of the seal liners showed the track widths in the misaligned state are significantly wider, due to stronger wiping effects with maximum differences of between 52.94% and 97.60% being recorded. However, with a larger track width, the track depth is significantly lower. This is because the sealing rings around the circumference do not have a constant surface pressure (as with the ideally aligned seal) and the area over which the contact pressure is distributed is larger on the liner. For the first and last sealing rings (LS4 and LS1), the difference in the liner track wear depths was found to be close to two orders of magnitude.

It is expected the results of this experimentation can used for the validation of numerical models on predicting the behaviour of rotary type lip seals for a submerged tidal turbine. Also, future work will investigate the performance of the seals under a transient misalignment between 1° and $-1°$.

5. Acknowledgements

This work forms part of the project TAOIDE which is funded by the European Union's H2020 research and innovation programme under the grant agreement number 727465.

References

[1] K. Fang, Y. Zhou, S. Wang, R. Ye, S. Guo, Assessing national renewable energy competitiveness of the G20: A revised Porter's Diamond Model, Renewable and Sustainable Energy Reviews 93 (May) (2018) 719–731. doi:10.1016/j.rser.2018.05.011.

[2] B. Hand, A. Cashman, Aerodynamic modeling methods for an offshore vertical axis wind turbine : A comparative study, Renewable Energy 129 (2018) 12–31. doi:10.1016/j.renene.2018.05.078.

[3] E. Segura, R. Morales, J. A. Somolinos, A. López, Techno-economic challenges of tidal energy conversion systems: Current status and trends, Renewable and Sustainable Energy Reviews 77 (April) (2017) 536–550. doi:10.1016/j.rser.2017.04.054.

[4] B. Hand, G. Kelly, A. Cashman, Aerodynamic design and performance parameters of a lift-type vertical axis wind turbine: A comprehensiv, Renewable and Sustainable Energy Reviews 139 (December 2019) (2021) 110699. URL https://doi.org/10.1016/j.rser.2020.110699

[5] A. López, J. L. Morán, L. R. Núñez, J. A. Somolinos, Study of a cost model of tidal energy farms in early design phases with parametrization and numerical values. Application to a second-generation device, Renewable and Sustainable Energy Reviews 117 (October 2019) (2020). doi:10.1016/j.rser.2019.109497.

[6] N. Erdogan, D. B. Murray, J. Giebhardt, M. Wecker, J. Donegan, Real-time hardware emulation of a power take-off model for grid-connected tidal energy systems, 2019 IEEE International Electric Machines and Drives Conference, IEMDC 2019 (727465) (2019) 1368–1372. doi:10.1109/IEMDC.2019.8785358.

[7] B. Hand, D. B. Murray, N. Erdogan, J. Murphy, P. Cronin, Development of a test setup for bearings and seal lifetime testing for a tidal energy application, in: International Conference on Ocean Energy, 2021, pp. 1–3.

[8] R. J. Wood, A. S. Bahaj, S. R. Turnock, L. Wang, M. Evans, Tribological design constraints of marine renewable energy systems, Philosophical Transactions of the Royal Society A: Mathematical, Physical and Engineering Sciences 368 (1929) (2010) 4807–4827. doi:10.1098/rsta.2010.0192.

[9] P. Qian, B. Feng, H. Liu, X. Tian, Y. Si, D. Zhang, Review on configuration and control methods of tidal current turbines, Renewable and Sustainable Energy Reviews 108 (July 2018) (2019) 125–139. doi:10.1016/j.rser.2019.03.051. URL https://doi.org/10.1016/j.rser.2019.03.051

[10] B. Hand, G. Kelly, A. Cashman, Structural analysis of an offshore vertical axis wind turbine composite blade experiencing an extreme wind load, Marine Structures 75 (September 2020) (2020) 102858. doi:10.1016/j.marstruc.2020.102858.

[11] A. Ebrahimi, Advances in Modelling and Control of Wind and Hydrogenerators, 2020. doi:10.5772/intechopen.77988.

[12] Q. Xu, W. Li, Y. Lin, H. Liu, Y. Gu, Investigation of the performance of a stand-alone horizontal axis tidal current turbine based on in situ. Ocean Engineering 113 (2016) 111–120. URL http://dx.doi.org/10.1016/j.oceaneng.2015.12.051

[13] S. H. Lee, S. S. Yoo, D. E. Kim, B. S. Kang, H. E. Kim, Accelerated wear test of FKM elastomer for life prediction of seals, Polymer Testing 31 (8) (2012) 993–1000. doi:10.1016/j.polymertesting.2012.07.017. URL http://dx.doi.org/10.1016/j.polymertesting.2012.07.017

[14] Y. Nakanishi, T. Honda, Y. Nakashima, H. Higaki, Shaft seal for separation of water and air with low frictional torque, Tribology International 94 (2016) 437–445. doi:10.1016/j.triboint.2015.10.007. URL http://dx.doi.org/10.1016/j.triboint.2015.10.007

[15] T. Honda, K. Kasamura, Y. Nakashima, H. Higaki, Y. Nakanishi, Low-friction shaft seal composed of bio-inspired materials covering low-speed range under water environment, Proceedings of the Institution of Mechanical Engineers, Part J: Journal of Engineering Tribology 232 (1) (2018) 36–42. doi:10.1177/1350650117738702.

[16] B. F. De Cal, Application of vibration monitoring to the detection of early misalignment and rub failures in a tidal turbine, Technology and Economics of Smart Grids and Sustainable Energy 4 (1) (2019) 1–11. doi:10.1007/s40866-019-0065-1.

[17] F. X. Borras, R. van den Nieuwendijk, V. Ramesh, M. B. de Rooij, D. J. Schipper, Stern tube seals operation: A practical approach, Advances in Mechanical Engineering 13 (2) (2021) 1–14. doi:10.1177/1687814021994404.

[18] SKF - Simplex sterntube seals. URL https://www.skf.com/group/industries/marine/simplex-and-skf-seals/seals/simplex-sterntube-seals

[19] KELLER, Series 23SY/25Y - Piezoresistive Pressure Transmitter Piezoresistive, Tech. rep. (2014).

[20] H2020 TAOIDE Subsystem Test Data (2021). doi:10.5281/zenodo.4710693. URL https://zenodo.org/record/4710693{#}.Ya5sjtDP3ct